Materials Science & Engineering A 605 (2014) 73–79

Contents lists available at ScienceDirect

Materials Science & Engineering A

journal homepage: www.elsevier.com/locate/msea

Influence of pre-strain on de-twinning activity in an extruded AM30 magnesium alloy

D. Sarker, J. Friedman, D.L. Chen*

Department of Mechanical and Industrial Engineering, Ryerson University, 350 Victoria Street, Toronto, Ontario M5B 2K3, Canada

ARTICLE INFO

Article history:
Received 15 February 2014
Received in revised form
4 March 2014
Accepted 12 March 2014
Available online 19 March 2014

Keywords:
Pre-strain
Re-compression
Twinning
De-twinning
Texture

ABSTRACT

This study was aimed at examining the compressive deformation behavior of an extruded AM30 alloy along the normal direction (ND) after different amounts of pre-strain along the extrusion direction (ED), with a focus on the strain hardening behavior, texture evolution, and deformation mechanisms. Compressive loading directly in the ND gave a slip-dominated flow behavior due to the presence of two sets of basal textures with *c*-axes aligned almost parallel to the ND, which was unfavorable for extension twinning. In the two-step ED–ND compression, the compressive yield strength decreased, while the ultimate compressive strength increased with increasing pre-strain. At the lower pre-strain levels two hardening stages of B and C occurred, while three hardening stages of A, B and C were present at the higher pre-strain levels. The peak value between stages B and C and the slope of strain hardening rate in stage B linearly decreased with increasing pre-strain. The phenomenon of de-twinning (or back-twinning) was observed, and the de-twinning activity decreased with increasing pre-strain in the ED while keeping the re-compression amount in the ND constant. Texture measurements revealed that the *c*-axes of hcp unit cells were always rotated towards the anti-compression direction, regardless of compression in the ED or ND. Texture weakening was achieved via the pre-compression in the ED and subsequent re-compression in the ND.

1. Introduction

Lightweighting of ground vehicles is today considered one of the most important strategies to improve fuel economy and reduce climate-changing and environment-damaging emissions [1–7]. It has been reported that the fuel efficiency of passenger vehicles can be enhanced by 6–8% for each 10% reduction in weight [8–10]. Thus magnesium alloys, as the lightest structural metallic materials, have recently drawn a lot of interest in the transportation industry to reduce the weight of vehicles due to their high strength-to-weight ratio, dimensional stability, and good machinability and recyclability. Wrought magnesium alloys have in general better tensile properties [11,12] and fatigue resistance [13–19] compared to cast magnesium alloys [20,21]. However, wrought magnesium alloys normally form a strong texture during manufacturing processes and exhibit a high degree of anisotropy and poor room temperature formability due to the limited slip systems in the hexagonal close-packed (hcp) crystal structure and the polar characteristics of deformation twinning.

During the manufacture of magnesium components (via rolling, leveling, coiling, bending, stretching, etc.) the change in strain path could have a significant influence on the mechanical behavior of magnesium alloys. The flow stress may increase or decrease when such alloys are subjected to strain reversals [9,22,23]. It is therefore important to identify the effect of reversing the strain path on the stress–strain response, as well as the role of twinning and de-twinning in bringing this about. The reverse motion of $\{10\bar{1}2\}$ twin boundaries or de-twinning was observed by Molnár et al. [24], during successive compression of a hot-rolled AZ31 alloy at 3.5% strain along the rolling direction (RD) and then along the normal direction (ND). During the initial compression along the RD, $\{10\bar{1}2\}$ twinning was the main deformation mode, whereas a twin-free microstructure was observed after subsequent compression along the ND which restored the initial shape of the sample. Xin et al. [25] examined the plastic deformation behavior of a hot-rolled AZ31 alloy under 6 passes of plain compression along the transverse direction (TD) and ND alternatively, and reported that at 10% compression along the TD most grains were nearly twinned and extension twinning took place during subsequent compression along the ND without any de-twinning. However, Proust et al. [26] studied the effect of strain path change on twinning and de-twinning where an AZ31-H24 alloy was pre-strained in plane and then reloaded along the through-thickness direction, and observed that the twinned region of the grain that had been created during the loading phase of the deformation was allowed to shrink until it disappeared totally and

* Corresponding author. Tel.: +1 416 979 5000x6487; fax: +1 416 979 5265.
E-mail address: dchen@ryerson.ca (D.L. Chen).

http://dx.doi.org/10.1016/j.msea.2014.03.046
0921-5093/

the grain was then constituted entirely of matrix. Similar results of de-twinning were observed by Brown et al. [27] in rolled beryllium which was initially deformed in-plane and then in the through-thickness direction.

Twinning and de-twinning phenomena in hcp materials such as magnesium [24], beryllium [27] and zirconium [28] have been reported. The occurrence of twinning and de-twinning has a significant impact on the mechanical properties of magnesium and its alloys [24,26,27]. The de-twinning of Mg alloys has been reported to increase fatigue resistance [29,30], improve tensile and compressive properties [20,31], and decrease tension–compression yielding asymmetry [32]. Thus Mg alloys have been recently referred to as a smart material [24]. However, it is unclear how de-twinning occurs in a previously twinned sample with a change of strain path, especially how the pre-strain amount affects the subsequent strain hardening behavior, de-twinning tendency, and the associated texture change. The objective of this study was, therefore, to explore the relationship between the hardening behavior, texture evolution, and de-twinning in an extruded AM30 alloy upon changing the strain path.

2. Experimental

AM30 extruded magnesium alloy was selected in the present study. Rectangular samples of 5 mm × 4 mm × 6 mm (ED × TD × ND) dimensions were chosen for the compression test. Samples were first pre-strained along the ED at different strain levels of 2.1%, 3.7%, 5.4% and 7.9% (referred to as 2.1%ED, 3.7%ED, 5.4%ED, and 7.9%ED, respectively) using a computerized Instron machine at a strain rate of $1.25 \times 10^{-4}\ s^{-1}$ and at room temperature. Pre-strained rectangular samples were subjected to recompression along the ND until failure. To observe the microstructural change and texture evolution, some pre-deformed samples were re-deformed to a strain amount of 3.7% along the ND. The reason for choosing this strain amount for re-compression was based on the observations that at this strain level along the ED grains were subjected to extensive twinning [33,34]. It should be noted that in the strain-related evaluation (i.e., strain amounts, stress–strain curves and strain-hardening rates), the machine deformation was eliminated using a calibration curve to arrive at the actual or net strain values of all test samples, as mentioned above. For the microstructural characterization, the deformed or re-deformed samples were cut along the compression axis using a slow diamond cutter, cold-mounted, ground up to a grit of #1200, and polished with 6, 3, and 1 μm diamond paste, respectively, and etched using an acetic picral solution containing 4.2-g picric acid, 10-ml acetic acid, 10-ml H_2O, and 70-ml ethanol to examine the evolution of deformation twins during compression. Texture was determined using a PANalytical X-ray diffractometer (XRD) by measuring a set of five incomplete pole figures ({0001}, $\{10\bar{1}0\}$, $\{10\bar{1}1\}$, $\{11\bar{2}0\}$, $\{10\bar{1}3\}$) between $\Psi = 0$ to 75° in a back reflection mode using Cu K_α radiation at 45 kV and 40 mA. Then the pole figures were evaluated using MTEX toolbox [35]. It should be noted that defocusing may occur due to the rotation of the XRD sample holder during the texture measurement [36], which was subsequently corrected using experimentally determined data from the diffraction of magnesium powders which were assumed to be texture-free.

3. Results and discussion

The true stress–true strain behavior of the samples that were subjected to different amounts of pre-strain along the ED is shown in Fig. 1(a), where the re-compression was conducted along the ND, as denoted by *x*%ED–ND, where *x* indicates the pre-strain amount after excluding the machine deformation. It is of interest to see that a marked change in the shape of the true stress–true strain curve occurred. Without pre-straining along the ED, the compression in the ND showed the true stress–true strain curve appeared similar to a slip dominated one (e.g., for the fcc and/or bcc metals) with a higher yield stress of ~175 MPa, which decreased to ~91 MPa when different amounts of pre-strains along the ED were applied. With increasing pre-strain from 2.1% ED, 3.7%ED, 5.4%ED, and 7.9%ED, the skewed curve shape gradually became more obvious. When the pre-strain reached about 5.4–7.9%, the true stress–true strain curve looked like a twin dominated one. A slight increase in ultimate compressive strength and decrease in fracture strain with increasing pre-strain amount were also observed. Again, such a sigmoidal shape is consistent with the twin formation, and the subsequent twin–twin and twin–dislocation interactions, leading to the distinctive strain hardening in compression [31,37].

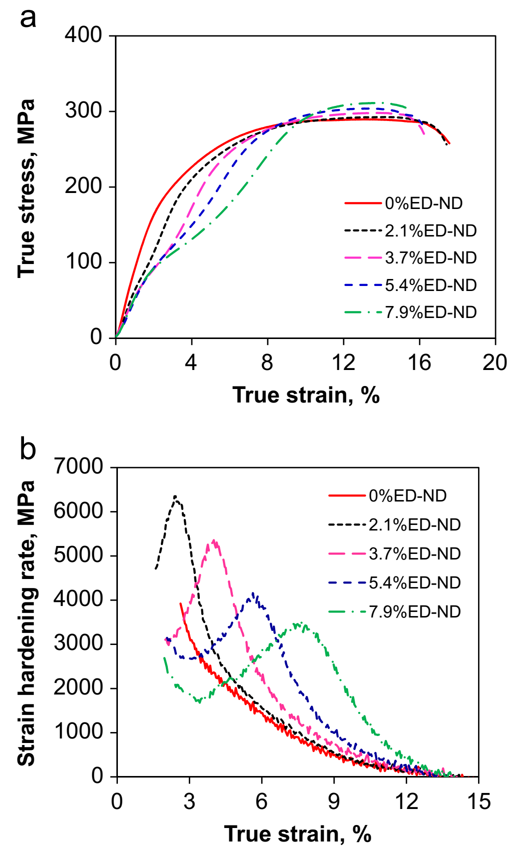

Fig. 1. (a) True stress–true strain curves and (b) strain hardening rate vs. true strain obtained in re-compression along the ND, after pre-compression along the ED to various strain levels.

After re-compression along the ND direction, the strain hardening rate θ ($= d\sigma/d\varepsilon$, where σ is true stress) as a function of true strain ε, is plotted in Fig. 1(b). It should be noted that as there was no rising strain hardening rate present in the tensile deformation [41] (like stage B in the compressive deformation in Fig. 1(b)), θ and $d\theta/d\varepsilon$ were evaluated only from the compressive true stress–strain curves in this study. In the absence of pre-straining, compression along the ND resulted in a direct decrease in the hardening curve, which was equivalent to stage III hardening followed by stage IV hardening in the tensile deformation [38–40]. In the presence of pre-strain in the ED, different stages of strain hardening could be distinguished. In the case of the lower pre-strain level of 2.1% and 3.7%, two distinct stages (i.e., stages B